Disruption of *Plasmodium falciparum* development by antibodies against a conserved mosquito midgut antigen

Rhoel R. Dinglasan*†, Dario E. Kalume‡§, Stefan M. Kanzok*, Anil K. Ghosh*, Olga Muratova¶, Akhilesh Pandey‡, and Marcelo Jacobs-Lorena*†

*Department of Molecular Microbiology and Immunology, Malaria Research Institute, Johns Hopkins Bloomberg School of Public Health, 615 North Wolfe Street, Baltimore, MD 21205; ‡Institute of Genetic Medicine, Johns Hopkins School of Medicine, 733 North Broadway, Baltimore, MD 21205; and ¶Malaria Vaccine Development Unit, National Institute of Allergy and Infectious Diseases, National Institutes of Health, 5640 Fishers Lane, Rockville, MD 20852

Edited by Abdu F. Azad, University of Maryland, Baltimore, MD, and accepted by the Editorial Board June 21, 2007 (received for review March 10, 2007)

Malaria parasites must undergo development within mosquitoes to be transmitted to a new host. Antivector transmission-blocking vaccines inhibit parasite development by preventing ookinete interaction with mosquito midgut ligands. Therefore, the discovery of novel midgut antigen targets is paramount. Jacalin (a lectin) inhibits ookinete attachment by masking glycan ligands on midgut epithelial surface glycoproteins. However, the identities of these midgut glycoproteins have remained unknown. Here we report on the molecular characterization of an *Anopheles gambiae* aminopeptidase N (AgAPN1) as the predominant jacalin target on the mosquito midgut luminal surface and provide evidence for its role in ookinete invasion. α-AgAPN1 IgG strongly inhibited both *Plasmodium berghei* and *Plasmodium falciparum* development in different mosquito species, implying that AgAPN1 has a conserved role in ookinete invasion of the midgut. Molecules targeting single midgut antigens seldom achieve complete abrogation of parasite development. However, the combined blocking activity of α-AgAPN1 IgG and an unrelated inhibitory peptide, SM1, against *P. berghei* was incomplete. We also found that SM1 can block only *P. berghei*, whereas α-AgAPN1 IgG can block both parasite species significantly. Therefore, we hypothesize that ookinetes can evade inhibition by two potent transmission-blocking molecules, presumably through the use of other ligands, and that this process further partitions murine from human parasite midgut invasion models. These results advance our understanding of malaria parasite–mosquito host interactions and guide in the design of transmission-blocking vaccines.

glycan | malaria | mass spectrometry | transmission-blocking vaccine

An effective and economical control strategy against malaria is lacking. This devastating arthropod-borne disease is caused by the protozoan parasite *Plasmodium*, which must complete development in the *Anopheles* mosquito before transmission to a new host (1, 2). *Plasmodium* ookinetes form in the mosquito midgut luminal bloodmeal and migrate to the periphery where they are thought to recognize midgut ligands. Recognition is followed by cell invasion and differentiation into oocysts between the midgut basal cell surface and the basal lamina. Each oocyst releases thousands of sporozoites that invade the mosquito salivary glands and are delivered to a vertebrate host during a succeeding bloodmeal. Clearly, the ookinete-to-oocyst transition is crucial for successful parasite establishment in the mosquito and, therefore, represents the best paradigm to develop novel interventions. One promising approach is the use of antivector malaria transmission-blocking vaccines (TBV) that prevent ookinete-to-oocyst transition by targeting mosquito midgut ligands that mediate parasite cell adhesion as opposed to classical TBVs, which target surface molecules on parasite sexual stages (3).

Oligosaccharides on gut microvillar glycoconjugates have been implicated as both receptors for microbial attachment and as a protective barrier against pathogens in both vertebrates and invertebrates (4–7). In the mosquito, midgut microvilli (MMV) glycoconjugates have been shown to play a role in the establishment of parasite infections. Glycans, such as *N*-acetylgalactosamine (GalNAc), or lectins, such as jacalin, reduce parasite attachment to the mosquito midgut (8). Accordingly, a monoclonal antibody (mAb) to MMV glycans blocks parasite development completely (9). This mAb recognizes *N*-acetyllactosamine type II disaccharides commonly found on *N*- and *O*-glycans of various glycoconjugates, including glycolipids (10). Glycosaminoglycans (GAGs) on gut proteins also can act as potential ligands because several ookinete molecules bind to heparin *in vitro* (11). Protein epitopes of MMV glycoproteins also have been shown to be effective transmission-blocking targets (12, 13). However, to date, the identities of these glycoproteins remain unknown.

Here, we report on the use of jacalin-affinity chromatography and tandem MS to identify an abundant, O-glycosylated MMV glycoprotein. We provide evidence for its utility as an effective, conserved antivector transmission-blocking antigen and as a molecular tool for dissecting ookinete adhesion strategies in the mosquito.

Results

Identification of O-Glycosylated Midgut Microvillar Proteins by Lectin-Affinity Chromatography and Protein Sequencing. Three predicted aminopeptidases (APN; E.C. 3.4.11.2), an *O*-glycoside hydrolase (E.C. 3.2.1) and a protein of unknown function were identified from the 800 mM galactose (Gal) eluate (Fig. 1*a* and Table 1). *Anopheles gambiae* aminopeptidase N (AgAPN1) contains a well conserved gluzincin aminopeptidase motif (Fig. 1*b*). The prototypical insect gluzincin aminopeptidase N motif, which starts at Gly^{304} on AgAPN1, **GAMENWG**X_{31}-**HE**X_2**H**X_{17}-**E** (where X is any amino acid) is associated with Zn^{2+} coordination, substrate binding, and catalysis (14). AgAPN1 is predicted to have a glycosylphosphatidyl

Author contributions: R.R.D. designed research; R.R.D., D.E.K., S.M.K., A.K.G., and O.M. performed research; D.E.K. and A.P. contributed new reagents/analytic tools; R.R.D. and D.E.K. analyzed data; and R.R.D. and M.J.-L. wrote the paper.

The authors declare no conflict of interest.

This article is a PNAS Direct Submission. A.F.A. is a guest editor invited by the Editorial Board.

Abbreviations: AgAPN1, *Anopheles gambiae* aminopeptidase N; TBV, transmission-blocking vaccines; MMV, midgut microvilli; GAG, glycosaminoglycan; APN, aminopeptidase; GPI, glycosylphosphatidyl inositol; PAb, polyclonal antibody; PBF, post blood-feeding; Gal, galactose; ds, double-stranded.

†To whom correspondence may be addressed. E-mail: rdinglas@jhsph.edu or mlorena@jhsph.edu.

§Present address: Fundação Oswaldo Cruz, Instituto Oswaldo Cruz, Laboratório de Epidemiologia Molecular de Doenças Infecciosas, Avenida Brasil, 4365, Manguinhos, RJ 21040-900, Rio de Janeiro, Brazil.

This article contains supporting information online at www.pnas.org/cgi/content/full/0702239104/DC1.

© 2007 by The National Academy of Sciences of the USA

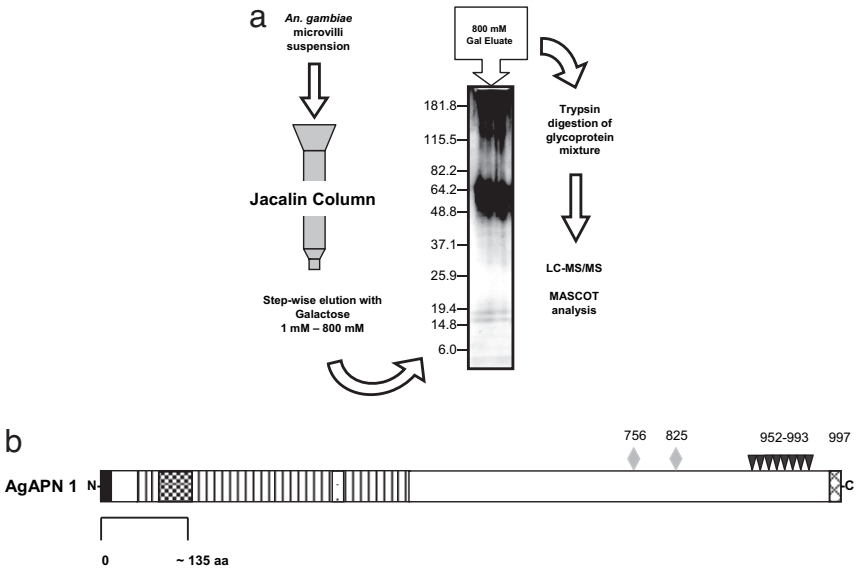

Fig. 1. Characterization of O-glycosylated MMV glycoproteins by jacalin chromatography and protein sequencing. (*a*) Schematic of the jacalin-affinity chromatography and tandem MS approach. Solubilized microvilli were loaded onto the jacalin column and eluted with Gal. An aliquot of the 800 mM Gal eluate was fractionated by electrophoresis and silver-stained. The remaining sample was subjected to proteomic analysis (Table 1). (*b*) Predicted structure and glycosylation sites of AgAPN1. Black rectangle, predicted signal sequence; vertically hatched rectangles, peptidase M1 family domains; checkered box, antibody epitopes; stippled box, gluzincin motif; cross-hatched box, C-terminal GPI anchor. Predicted glycosylation sites are as follows: filled triangles, O-linked glycan,; filled diamonds, GAG modification site. Amino acid position numbers for the corresponding sites are as indicated. The diagram is drawn to scale. Note that AgAPN1 is predicted to have multiple *O*-glycan and GAG modification sites that are ligands for jacalin and, presumably, ookinete micronemal proteins, respectively (see text for details).

inositol (GPI) anchor (Fig. 1*b*) and a mucin-like domain composed of 25 Ser/Thr-rich motifs that are predictive of O-glycosylation sites ($Thr^{952–993}$). AgAPN1 also has two predicted GAG sites at Thr^{756} and Thr^{825}, which may act as sites for ookinete binding (ref. 11 and R.R.D., unpublished results). Repeated analysis of separate jacalin chromatography fractions by liquid chromatography/tandem MS suggested that AgAPN1 represents the most abundant species in the mixture. The *O*-glycoside hydrolase is an enzyme that is involved in carbohydrate metabolism (http://afmb.cnrs-mrs.fr/CAZY) with known activities in mosquitoes (15–17). Based on the high affinity with which AgAPN1 binds to jacalin, its relative abundance in the mixture and the number of predicted O-linked and GAG sites, we chose to examine this glycoprotein further.

AgAPN1 Is Expressed in the Midguts of Sugar-Fed and Blood-Fed Mosquitoes. RT-PCR analysis of midgut mRNA suggests that *AgAPN1*-specific transcripts are constitutively expressed in midguts of sugar-fed and blood-fed mosquitoes (Fig. 2*a*).

Rabbit polyclonal antibodies (PAbs) to AgAPN1 recognize a single protein band at ≈125 kDa and a protein doublet at ≈60 kDa [Fig. 2*b* and supporting information (SI) Fig. 4*a*]. The higher M_r band is close to the predicted full-length AgAPN1 (113.5 kDa). Differences in apparent versus predicted M_r can be in part attributable to the presence of the O-linked glycans on AgAPN1. The lower M_r bands that also are present in guts from blood-fed mosquitoes may correspond to degradation products or cross-reacting proteins. Immunofluorescence microscopy suggests that AgAPN1 localizes to the luminal MMV in guts from sugar-fed and blood-fed mosquitoes (Fig. 2*c C* and *D*) and remains associated with the MMV–bloodmeal interface during ookinete invasion.

Immunoblot analysis of the supernatant and pellet fractions of phosphotidylinositol-specific phospholipase C (PI-PLC)-treated MMV solutions suggest the presence of a GPI anchor on AgAPN1 and that recognition of AgAPN1 is midgut-specific (SI Fig. 4). GPI linkage along with previous evidence that jacalin inhibits ookinete adhesion to MMV (8) support the observation of AgAPN1 localization to the apical midgut surface.

A comparative immunoblot analysis of midgut lysates from sugar-fed *Anopheles stephensi*, *Anopheles arabiensis*, *Anopheles freeborni*, and *A. gambiae* detected the predicted 125-kDa AgAPN1 in all four species (Fig. 2*d*). An aminopeptidase of corresponding relative mobility was described previously in *A. stephensi* (18), suggesting that PAbs may recognize an ortholog of AgAPN1. Additional faster migrating bands also were consistently detected in a species-specific manner. It is not clear whether these bands are proteolytic products.

α-AgAPN1 PAbs and Transmission-Blocking mAb MG96 Recognize Similar Midgut Glycoproteins. α-AgAPN1 PAbs recognize *AgAPN1* products in the 800 mM Gal eluent only, confirming the high affinity of jacalin for AgAPN1 (Fig. 2*e Upper*). The recognition of the two AgAPN1 products is remarkably similar to the banding profile observed for the transmission-blocking and anti-glycan mAb MG96 (9). MG96 appears to recognize a high M_r glycoprotein that may correspond to AgAPN1 (Fig. 2*e Lower*). As shown previously, the diffuse signals generated by MG96 are caused by its recognition

Table 1. Tandem MS identification of *Anopheles gambiae* midgut microvilli glycoproteins isolated by jacalin-affinity chromatography

NCBI no.	Ensembl	Annotation	Mascot score	Predicted M_r, kDa	Additional features
gi_31228112	ENSANGP00000003366	Alanyl aminopeptidase N (AgAPN1)	188	113.5	Chromosome 2L, GPI anchor, Zn-metallopeptidase domain
gi_31241511	ENSANGP00000007943	Alanyl aminopeptidase N (AgAPN2)	97	104.7	Chromosome 2R, Zn-metallopeptidase domain, no TMD or GPI anchor
gi_31210729	ENSANGP00000001203	Alanyl aminopeptidase N (AgAPN3)	59	84.9	Chromosome 2L, Zn-metallopeptidase domain, no TMD or GPI anchor
gi_31230994	ENSANGP00000024978	*O*-glycosyl hydrolase homolog	52	61.5	Chromosome 2R, glycoside hydrolase family 31, no TMD or GPI anchor, similar to α-galactosidases
gi_31210671	ENSANGP00000013165	Unknown function	49	19.7	Chromosome 2L, N-terminal TMD

NCBI, National Center for Biotechnology Information; TMD, transmembrane domain. Mascot score, probability-based molecular weight search (MOWSE) score. Score, $-10 \times \log 10(P)$, where P is the probability that the observed match of a protein with the nonredundant database is a random event. The protein scores were ranked, and individual ion scores >51 indicated significant identity ($P < 0.05$).

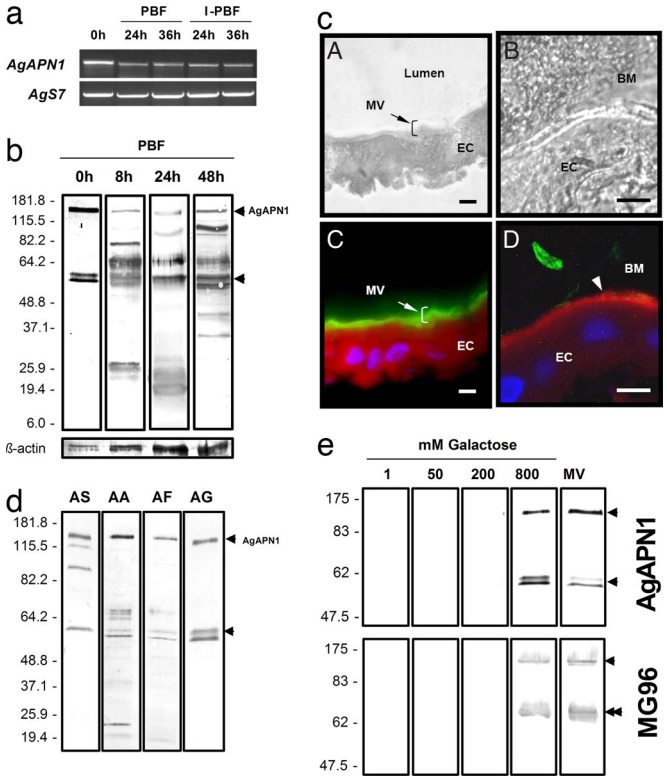

Fig. 2. AgAPN1 expression and recognition by α-AgAPN1 PAbs. (*a*) RT-PCR analysis of *AgAPN1* expression in guts from sugar-fed (0 h), blood-fed (24 h and 36 h PBF), and infected blood-fed (I-PBF) *A. gambiae*. Mosquito ribosomal S7 gene (*AgS7*) was used as a loading control. (*b*) Immunoblot of midgut lysates prepared at the indicated time points after a noninfected bloodmeal. Antibody to actin was used as a loading control. The upper arrowhead indicates the expected size of the predicted full-length AgAPN1 product. Preimmune serum does not recognize mosquito midgut antigens (SI Fig. 4). The lower arrowhead indicates a presumed degradation product of AgAPN1. (*c*) Immunofluorescence analysis of midgut cross-sections from *A. gambiae* fed on sugar (*A* and *C*) or on *P. falciparum*-infected blood (*B* and *D*) and stained with α-AgAPN1 PAb. Bright-field images of midguts from sugar-fed (*A*) and infected blood-fed (24 h PBF) (*B*) mosquito. *C* shows a fluorescence image of the same field as in *A* and shows α-AgAPN1 PAb staining of the microvilli (MV; arrow/bracket) as detected by FITC-labeled secondary antibody (green) with Evans blue as a counterstain (red). *D* is a fluorescence image of the same field as in *B*. The ookinete was stained with anti-Pfs25 antibody (green). α-AgAPN1 PAb stains the midgut MV–bloodmeal interface (arrowhead red). Note that AgAPN1 is present on the MMV during ookinete invasion. EC, epithelial cell; BM, bloodmeal. DAPI-stained nuclei appear blue. (Scale bar, ≈100 μm.) (*d*) Comparative immunoblot analysis of whole midgut lysates from *A. stephensi* (AS), *A. arabiensis* (AA), *A. freeborni* (AF), and *A. gambiae* (AG) with α-AgAPN1 PAb suggest that α-AgAPN1 PAbs recognizes a conserved midgut molecule across different malaria insect vectors. (*e*) Immunoblot analyses of glycoproteins in fractions eluted from the jacalin column with the Gal concentration (mM) indicated at the top of each lane. Blots were probed with α-AgAPN1 PAb (*Upper*) or the anti-glycan mAb MG96 (9) (*Lower*). MV, microvilli-enriched fraction (column input). Upper arrowhead indicates the predicted full-length AgAPN1 detected by both antibodies, whereas the lower arrowhead indicates protein doublet recognition specific for α-AgAPN1 PAb. MG96 recognizes a protein doublet (double arrowhead) with a different mobility relative to size markers than the doublet in *Upper*. Position of migration of molecular mass markers (kDa) is shown on the left of each immunoblot.

of glycans (9). MG96 stains a lower M_r band (double arrowhead in Fig. 2*e Lower*) that has a different mobility (relative to size markers) than the protein doublet in Fig. 2*e Upper*. MG96 may recognize *O*-glycans on either AgAPN2 or AgAPN3 (Table 1) or another glycoprotein. Because jacalin inhibits ookinete attachment (8), as well as competitively inhibits MG96 binding (10), we considered the possibility that α-AgAPN1 PAbs also may impede ookinete access to the mosquito midgut.

α-AgAPN1 PAbs Confer Transmission-Blocking Immunity Against both *Plasmodium berghei* and *Plasmodium falciparum*. We found that 100 μg/ml of α-AgAPN1 PAbs significantly reduced *P. berghei* oocyst formation in *A. gambiae* (75% inhibition, $P < 0.0001$) (Fig. 3*a*). Similar inhibition of *P. berghei* development was observed in *A. stephensi* (data not shown). At 400 μg/ml and 800 μg/ml, the median inhibition increased up to 79% ($P = 0.0015$) and 87% ($P < 0.0001$), respectively (Fig. 3*a*). These results were mirrored in transmission-blocking experiments against *P. falciparum* (Fig. 3*c* and SI Fig. 5).

Fab Fragments of α-AgAPN1 IgG Exhibited Decreased Transmission-Blocking Potential. To test whether inhibition of oocyst formation was attributable to steric hindrance by IgG molecules, α-AgAPN1 PAbs were digested with papain to produce monomeric Fab fragments. α-AgAPN1 Fab (100 μg/ml) did not confer inhibition (Fig. 3*a*). However, at 400 μg/ml and 800 μg/ml, inhibition increased up to 32% ($P = 0.2824$) and 78% ($P < 0.0001$), respectively (Fig. 3*a*). Because of its monovalency, Fab affinity generally is less than that observed for whole IgG. On the other hand, $F(ab')_2$ fragments exhibited inhibition levels equivalent to that of intact IgG at 100 μg/ml (80% inhibition, $P < 0.0001$; data not shown).

Plasmodium Ookinetes Can Use Multiple Ligands for Midgut Invasion. α-AgAPN1 PAbs, even at the highest concentration tested (Fig. 3*a*), did not confer complete inhibition of oocyst development, which is in contrast to previous studies using anti-midgut antibodies that could completely block parasite invasion (9, 13) presumably by blocking multiple targets. Therefore, we used a second effector molecule, the salivary gland and midgut peptide 1 (SM1), to determine whether parasite breakthrough was caused by alternate midgut recognition mechanisms via distinct receptors (i.e., not all ookinetes may use AgAPN1 as a cell invasion ligand).

SM1 is a 12-aa peptide that effectively blocks *P. berghei* development in *A. stephensi* (19, 20). However, SM1-mediated inhibition, although potent, is incomplete (between 60% and 70%). Proteomic analysis of SM1-bound proteins suggests that AgAPN1 is not recognized by SM1 (A.K.G., unpublished data). In addition, results from a competitive ELISA, using α-AgAPN1 PAb and SM1 as competitors for binding to midgut lysates, indicate that each molecule recognizes different ligands on the midgut surface (R.R.D., unpublished data). Therefore, we tested whether concomitant introduction of both effector molecules in a single infective bloodmeal would result in increased inhibition of parasite development. SM1 (100 μg/ml) injected (i.v.) into an infected mouse inhibited oocyst formation by 68% ($P = 0.0372$) (Fig. 3*b*). A single injection of both SM1 and α-AgAPN1 PAbs resulted in 95% inhibition ($P < 0.0001$) (Fig. 3*b*), which was significantly different from inhibition by SM1 alone ($P = 0.0007$).

α-AgAPN1 PAbs, but Not SM1, Confer Transmission-Blocking Immunity Against *P. falciparum*. We observed comparable transmission-blocking levels against *P. falciparum by using* 200 μg/ml of α-AgAPN1 PAb in both *A. stephensi* and *A. gambiae* (Fig. 3*c*). In contrast, 200 μg/ml of SM1 exhibited only partial inhibition of *P. falciparum* development in *A. stephensi* (up to 34%; data not shown). However, the effect was not statistically significant ($P = 0.091$).

Discussion

The ultimate goal for examining potential mosquito midgut antigens is to develop a global TBV that works against all human malaria parasites across different anopheline species. Unfortunately, progress has been slow given that transmission-blocking mosquito antigens have not been characterized. Our data ad-

MICROBIOLOGY

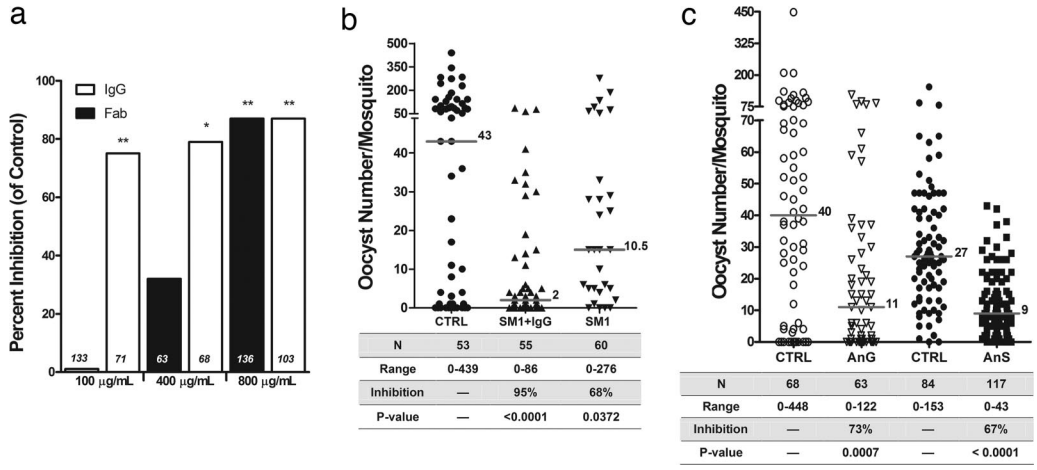

Fig. 3. α-AgAPN1 PAbs block *P. berghei* and *P. falciparum* development in mosquitoes. (*a*) α-AgAPN1 IgG and Fab fragments inhibit oocyst development in mosquitoes. *A. gambiae* mosquitoes were fed on *P. berghei*-infected mice that were passively immunized (i.v.) with α-AgAPN1 IgG or Fab. Numbers of mosquitoes analyzed are shown in the bottom of each column. Pooled data from three replicate experiments are shown. Asterisks denote significance values of $P < 0.05$ (*) and $P < 0.0001$ (**). (*b*) Salivary gland and midgut peptide 1 (SM1) and α-AgAPN1 IgG produces additive but incomplete transmission-blocking immunity. Note that these experiments could be performed only by using *P. berghei* because SM1 did not block significantly *P. falciparum* in our experiments (34% maximal inhibition, $P > 0.05$; results not shown). (*c*) α-AgAPN1 IgG inhibit *P. falciparum* development in *A. gambiae* (AnG) and *A. stephensi* (AnS). Mosquitoes were fed on *P. falciparum*-infected blood containing 200 μg/ml of α-AgAPN1 IgG. Control (CTRL) mosquitoes were fed on infected blood along with an equivalent concentration of preimmune rabbit IgG. Results represent pooled data from three independent experiments. (*b* and *c*) The horizontal bar and number indicate the median oocyst number per mosquito midgut for each IgG treatment group. The number of mosquitoes analyzed (*N*) and range in oocyst number are indicated in the table. Mosquito infection prevalence between control and treatment groups for all our transmission-blocking experiments did not differ significantly (ranging between 80% and 95% prevalence). Percentage inhibition = [(control median oocyst no. − experimental median oocyst no.)/control median oocyst no.)] × 100.

dress this gap in knowledge and provide evidence that AgAPN1 is a conserved, putative ligand for both murine and human *Plasmodium* ookinetes in diverse mosquito vectors.

Aminopeptidases as Agonists and Antagonists of *Plasmodium* ookinete Midgut Cell Invasion. Because jacalin has been shown to inhibit ookinete attachment (8), our identification of AgAPN1 suggests that this midgut glycoprotein mediates, directly or indirectly, parasite invasion of the gut. Although the N-terminal domain that was used for antibody production shares little homology with other proteins and mosquito midgut aminopeptidases (data not shown), we observed recognition of a ≈60-kDa doublet. This doublet may be a degradation or cleavage product of AgAPN1 that occurs during transit to the cell surface because it has been shown that midgut glycoproteins are cosecreted within the same vesicles as digestive enzymes (21). Coelution of this doublet from the jacalin column may be a result of molecular associations stemming from AgAPN1's proline-rich mucin domains, which can facilitate homodimer or heteromer associations (22, 23). At present, we do not know whether the other aminopeptidases we had identified mediate ookinete invasion of the midgut.

The activity of *A. gambiae* midgut aminopeptidases was reported to be highest during the early course (<24 h) of bloodmeal digestion (24) and that aminopeptidase activity is up-regulated specifically in response to a *P. berghei*-infected bloodmeal (25). However, our data along with recent microarray data did not show evidence that AgAPN1 was up-regulated in response to an infected bloodmeal (26). AgAPN1 is present during the ookinete traversal of the midgut [18–36 h post blood-feeding (PBF)], and antibodies against AgAPN1 clearly interfere with the ookinete-to-oocyst transition. However, it is unclear whether AgAPN1 operates directly as an adhesion ligand for ookinetes or whether its action is indirect, functioning as an enzyme that proteolytically activates a secreted ookinete invasion molecule. RNAi-mediated silencing of AgAPN1 may have addressed these issues. However, despite the injection of 400 ng to 5.4 μg of double-stranded (ds)AgAPN1 into the mosquito hemocoel upon eclosion or immediately before or after blood-feeding, AgAPN1 expression could not be silenced at the RNA or protein level (see *Materials and Methods* and SI Fig. 6). These results are in stark contrast to our success in silencing other midgut genes, for example, midgut glycosylating enzymes (R.R.D., unpublished results) and a serine protease inhibitor, SRPN6 (27). It is possible that the mRNAs for these midgut genes, in particular, are refractory to RNAi akin to that described for most of the neuronal mRNAs from *Caenorhabditis elegans* (28).

The Role of Antibody Size and Valency in α-AgAPN1 Inhibitory Activity. Higher amounts of α-AgAPN1 Fab are required to achieve inhibitory levels obtained with whole IgG or with $F(ab')_2$, which suggests that affinity and molecular size (i.e., steric effects) are the primary mechanisms involved in achieving blocking at the 100 μg/ml concentration. Both IgG and $F(ab')_2$ exhibit similar blocking activity at equivalent concentrations. This finding suggests that the rabbit Fc portion of the IgG, which can trigger the classical Fc-mediated complement pathway against *Plasmodium*, is not involved in the transmission-blocking effect observed in our studies, although the involvement of the alternate complement pathway cannot be ruled out. Moreover, the loss of the Fc, without corresponding loss of inhibitory activity, suggests that molecular size alone cannot explain the effect. It is likely that bivalency, inherent in $F(ab')_2$ (and IgG) molecules, increases the affinity for the cognate epitope, which leads to greater inhibitory efficiency. Alternatively, bivalent cross-linking of AgAPN1 may affect membrane fluidity at localized ookinete contact points, thereby preventing the reassortment of midgut molecules that has been observed during ookinete invasion (29). What is clear is that only modest amounts of antibody are required to confer transmission-blocking immunity. In general, antigen-specific IgG comprise between 1% and 5% of the total pool of PAb from immunized serum, suggesting that eliciting transmission-blocking antibody titers in humans is plausible.

Characterization of the Inhibitory Mechanism by Discrete Transmission-Blocking Molecules Reveals Heterogeneity in Ookinete Invasion for both Cloned and Direct Isolates of *Plasmodium*. Saturating α-AgAPN1 IgG concentrations and the coaddition of SM1 peptide with the IgG in a *P. berghei*-infective bloodmeal did not confer complete inhibition. If we assume that SM1 and α-AgAPN1 IgG recognize distinct midgut molecules, we then can interpret the combined inhibition result to be additive. SM1 blocks ≈70% of the total ookinete population, and α-AgAPN1 IgG blocks 70% of the remaining 30%. Therefore, we hypothesize that α-AgAPN1

PAb and SM1 have overlapping transmission-blocking activities against a majority of the ookinetes in the population. AgAPN1 and the SM1 epitope represent two discrete ligands for ookinetes on the midgut. Consequently, parasite breakthrough may indicate the presence of another ookinete ligand that is not masked by either effector molecule. We also observed that SM1 effectively blocks *P. berghei* development but not *P. falciparum* in the mosquito. In contrast, α-AgAPN1 IgG inhibits both parasite species effectively, implying that AgAPN1 has a conserved role in midgut cell invasion by ookinetes. Together, these data suggest that human and murine malaria parasite species use different midgut adhesion strategies. This is a compelling observation of species-specific midgut recognition mechanisms among *Plasmodium* sexual stages.

To distinguish the activities of SM1 and α-AgAPN1 IgG further, we isolated individual subclones from the parental *P. berghei* ANKA 2.34 stock by limiting dilution. Evidence suggests that at least one of several subclones is resistant to α-AgAPN1 PAb (S.M.K., unpublished results). This observation provides support for the idea that breakthrough is caused by alternate ligand recognition by a small subset of ookinetes. These results have two clear implications: (*i*) multiligand targeting will be required to achieve complete mosquito-based TBV-mediated immunity and (*ii*) the use of the *P. berghei* murine model for understanding ookinete invasion mechanisms may be unsuitable. The first implication is supported by previous studies that targeted multiple midgut protein antigens (13), or a conserved glycan ligand on several different proteins (9), both of which achieved complete inhibition of parasite development. The murine malaria model is widely used because it facilitates the analysis of parasite–host interactions. However, as the second implication underscores, our results provide an example of how discoveries emanating from the use of *P. berghei* may not be applicable directly to *P. falciparum.*

In conclusion, we report on a previously uncharacterized, conserved, mosquito-derived *P. falciparum* transmission-blocking antigen as a candidate for the development of such vaccines (3, 30). These experiments also have led to a fundamental discovery of *Plasmodium* species-specific midgut recognition mechanisms that advance our understanding of parasite development in mosquitoes and guide the design of transmission-blocking interventions.

Materials and Methods

Preparation of the Mosquito MMV-Enriched Suspension. MMV-enriched suspensions were prepared from *A. gambiae* (Keele, Staffordshire, U.K.) females as previously described (31). Microvilli were treated with *Bacillus* cereus phosphotidylinositol-specific phospholipase C (PI-PLC) (Sigma, St. Louis, MO) for 4 h at 37°C to assay for GPI linkage. Whole midgut lysates were prepared from mosquitoes as described previously (9).

Jacalin-Affinity Column Preparation and Chromatography. The affinity column was prepared by packing a jacalin-agarose suspension (Vector Laboratories, Burlingame, CA) in 175 mM Tris·HCl, pH 7.5 (buffer A). The column was washed with 10 bed volumes of buffer A and 1 bed volume of 50 mM Tris·HCl, pH 7.5 (buffer B). The MMV-enriched suspension was solubilized in 2 ml of buffer B supplemented with 10 mM EDTA, 5 mM DTT, and 2% wt/vol ASBC80 nondetergent sulfobetaine. The column was topped with 700 μl of 10 mM Hepes, pH 7.5, 0.15 M NaCl, 0.1 mM $CaCl_2$, and 0.08% sodium azide (buffer C) and incubated overnight at 4°C. Bound O-linked glycoproteins were eluted in fractions with stepwise increments of the eluting sugar Gal: 1 mM Gal, 50 mM Gal, 200 mM Gal, and 800 mM Gal in buffer C. The 800 mM Gal fractions were concentrated and desalted by Amicon filtration (Millipore, Billerica, MA). This procedure was repeated with an independent preparation. The glycoprotein mixture was denatured, reduced, and alkylated (32) followed by digestion with porcine-trypsin (Sigma) overnight at 37°C.

Sample Preparation for MS Analysis. Sample micropurification and preparation for liquid chromatography/tandem MS was performed as described (33). The sample was purified with a reversed-phase nanocolumn (GeLoad tip; Eppendorf, Hamburg Germany), acidified [formic acid to 5% (vol/vol) final concentration], and loaded on to an equilibrated nanocolumn packed with POROS Oligo R3 reversed-phase chromatography medium (Applied Biosystems, Foster City, CA). After washing with 5% formic acid, the peptides were eluted, dried down, and redissolved in 40 μl of mobile phase A [100% H_2O with 0.4% acetic acid and 0.005% heptafluorobutyric acid (vol/vol)], and loaded into the liquid chromatography/MS system.

MS Analysis. The purified sample was loaded online onto a fused silica capillary column (12 μm of YMC gel ODS-A). The peptides were separated with a linear gradient elution from 95% mobile phase A to 45% mobile phase B [90% acetonitrile with 10% H_2O, 0.4% acetic acid, and 0.005% heptafluorobutyric acid (vol/vol)] in 40 min. A potential of 2.7 kV was applied to the emitter in the ion source. The mass spectra were acquired on a Micromass-Waters (Manchester, U.K.) quadrupole time-of-flight (Q-TOF) API-US mass spectrometer equipped with an ion source (Proxeon Biosystems, Odense, Denmark). The acquisition and the deconvolution of data were performed on a MassLynx Windows NT PC data system (version 4). All spectra were obtained in positive-ion mode. The processed tandem MS spectra were searched against the nonredundant protein database (Ensembl, version 24, November 2004; ftp://ftp.ncbi.nih.gov/genbank/genomes/Anopheles gambiae/). Searches were performed with Mascot version 1.9 (34).

***In Silico* Analysis of AgAPN1.** The complete sequence of AgAPN1 was analyzed for predicted domain architecture and posttranslational modifications by using MotifScan (35), big-PI predictor (36), and Center for Biological Sequence Analysis prediction server (www.cbs.dtu.dk/services/) algorithms. The aglycosylated N terminus of AgAPN1 was analyzed for possible antigenic sites (37).

Cloning, Recombinant AgAPN1 Expression, and the Production of PAbs. The AgAPN1 primers (For2-pBAD, 5′-CACCGAACGCTACCGTCTGCCAACAA-3′) and AgAPN1 405R primer (5′-TGCCAGATATCTTCGCTCGCCATT-3′) were used to amplify a 403-bp product corresponding to the N terminus of AgAPN1 from our *A. gambiae* midgut cDNA library. The PCR product was cloned into the pBAD102/D-TOPO vector (Invitrogen, Carlsbad, CA) and expressed in bacteria. Rabbit PAb was generated against the purified ≈25 kDa recombinant protein (Washington Biotechnologies, Columbia, MD).

Semiquantitative RT-PCR. For RT-PCR, 1 μg of total midgut RNA ($n = 20$ females) collected from each time point after blood-feeding was reverse-transcribed following standard protocols. AgAPN1 transcript abundance was determined by using the primers AgAPN1–2233F (5′-ATTCGCTTGGCTGCTCGAACAAT-3′) and 2886R (5′- TATCCCATGAGCAGGTGAACCGT-3′). The amplified *A. gambiae* ribosomal protein (AgS7) product was used as a loading control (AgS7F, 5′- TGCTGCAAACTTCGGCTAT-3′ and AgS7R, 5′- CGCTATGGTGTTCGGTTCC-3′). Amplification using Herculase polymerase (Stratagene, La Jolla, CA) was performed as follows: 94°C for 2 min, 94°C for 45 s, 57°C for 45 s, and 72°C for 45 s with a final extension at 72°C for 10 min (30 cycles). Cloned PCR products were confirmed by DNA sequencing.

RNAi-Mediated Gene Silencing. dsRNA corresponding to AgAPN1 exons or untranslated regions (UTRs) as well as green fluorescent protein (GFP) were synthesized with specific primers (SI Table 2) with the Megascript RNAi kit (Ambion, Austin, TX). *A. gambiae* females (4–6 days old) were cold-anesthetized and intrathoracically inoculated with 400 ng, 800 ng, 1,600 ng, and 5,400 ng of dsAgAPN1

(single exon/UTR targets or a mixture of all dsRNAs). Inoculations were performed on adults immediately after eclosion, at 4 days old, or at 24 h PBF. As a control, age-matched female mosquitoes were inoculated with equivalent concentrations of dsGFP. Total RNA or protein was isolated from pools of five to eight mosquitoes per time point.

SDS/PAGE and Western Blot Analysis. MMV lysates or suspensions were loaded (10 μg per well) into 10% Tris-glycine gels. Transblots were probed with α-AgAPN1 PAbs (1:500) followed by alkaline phosphatase-conjugated goat anti-rabbit IgG secondary antibody (Promega, Madison, WI) and detection with CDP-Star substrate (PerkinElmer, Wellesley, MA).

Immunofluorescence Microscopy of Midgut Cross-Sections. Cryosections of midguts were fixed in methanol and blocked (PBS/3% BSA). Each section was probed with α-AgAPN1 PAbs (1:500) or α-Pfs25 mouse mAbs. PAbs were detected by an Alexa-488 or Texas-red-conjugated α-rabbit IgG secondary antibody (Invitrogen) in 0.02% Evans blue. For double-stained sections, α-Pfs25 antibodies were detected by Alexa-488-conjugated anti-mouse secondary antibody.

Fab and F(ab′)$_2$ Preparation from Rabbit Polyclonal IgG. α-AgAPN1 polyclonal IgG (2 mg) were digested with immobilized papain (Pierce) overnight at 37°C to obtain the respective Fab fragments. The digested products were purified over a protein A column. F(ab′)$_2$ fragments were produced by digestion of 2 mg of IgG with immobilized pepsin (Pierce) for 6 h at 37°C and purified as above. Purity of all IgG fragments was verified by gel electrophoresis and Coomassie staining.

***Plasmodium* Transmission-Blocking Assay in *Anopheles*.** *P. berghei* (ANKA 2.34) infection was maintained following approved protocols and regulatory standards. For mosquito infections, four to five naïve mice were inoculated (i.p.) with 20,000 blood-stage parasites and checked for gametocytemia and exflagellation 2–3 days postinoculation. Mice with matching parasitemia (<6%) and between one and two gamete exflagellations per ×20 field were anesthetized. Three sets of control mosquitoes (n = 75 per cup) in pint-size ice-cream cups were allowed to blood-feed on a mouse (one mouse per control and treatment set) for 15 min. The mice were taken off the cage and passively immunized (i.v.) with rabbit antibody (to give a final concentration of 100 μg/ml preimmune IgG or α-AgAPN1 PAb). The concentration of antibody in the mouse was estimated by using the total blood volume per gram weight of each immunized mouse at the time of manipulation (≈2 ml of total blood volume per 25 g of mouse). Each mouse was allowed to recover for 10–15 min under a warm blanket. Another set of three cups of treatment mosquitoes (n = 75 per cup) were allowed to blood-feed on the immunized mouse for 15 min. The midguts from mosquitoes were dissected 10 days PBF and stained with 0.2% mercurochrome. Oocyst numbers were measured by using a compound microscope. At least three independent experiments were performed for each treatment.

P. falciparum (NF54) gametocyte cultures (38) were harvested 15–17 days after initiation and brought up in normal human serum (Tennessee Association of Blood Banks, Memphis, TN) plus human red blood cells at 0.3% gametocytemia in a 50% hematocrit. Infective blood was delivered directly into warmed membrane feeders or mixed with control preimmune or α-AgAPN1 IgG (before delivery). The final concentration of IgG in a total volume of 260 μl of infective blood was 200 μg/ml. Mosquitoes were allowed to blood-feed for 20 min. Midgut infection was assessed at 8 days PBF as described above. Three independent replicate experiments were performed.

Statistical Analyses. Nonparametric statistical analysis was used to evaluate the difference in median oocyst intensity between experimental and preimmune IgG control groups (Mann–Whitney U test, one-tailed, α = 0.05) by using the STATVIEW 5.0 software (SAS Institute, Cary, NC).

We thank Dr. Patricia Strickler-Dinglasan, Dr. Carole Long, and Dr. Fidel Zavala for suggestions. R.R.D. is a Dmitri V. d'Arbeloff Postdoctoral Fellow in the Biological Sciences (Millipore Foundation) and National Research Service Award 5F32AI068212-02 recipient. This research was supported by National Institutes of Health Grants R01AI031478 and RR00052.

1. Barillas-Mury C, Kumar S (2005) *Cell Microbiol* 7:1539–1545.
2. Ghosh A, Edwards MJ, Jacobs-Lorena M (2000) *Parasitol Today* 16:196–201.
3. Carter R (2001) *Vaccine* 19:2309–2314.
4. Abraham EG, Jacobs-Lorena M (2004) *Insect Biochem Mol Biol* 34:667–671.
5. Dinglasan RR, Jacobs-Lorena M (2005) *Infect Immun* 73:7797–7807.
6. Tellam RL, Vuocolo T, Eisemann C, Briscoe S, Riding G, Elvin C, Pearson R (2003) *Insect Biochem Mol Biol* 33:239–252.
7. Rostand KS, Esko JD (1997) *Infect Immun* 65:1–8.
8. Zieler H, Garon CF, Fischer ER, Shahabuddin M (2000) *J Exp Biol* 203:1599–1611.
9. Dinglasan RR, Fields I, Shahabuddin M, Azad AF, Sacci JB, Jr (2003) *Infect Immun* 71:6995–7001.
10. Dinglasan RR, Valenzuela JG, Azad AF (2005) *Insect Biochem Mol Biol* 35:1–10.
11. Li F, Templeton TJ, Popov V, Comer JE, Tsuboi T, Torii M, Vinetz JM (2004) *J Biol Chem* 279:26635–26644.
12. Shahabuddin M, Lemos FJ, Kaslow DC, Jacobs-Lorena M (1996) *Infect Immun* 64:739–743.
13. Lal AA, Patterson PS, Sacci JB, Vaughan JA, Paul C, Collins WE, Wirtz RA, Azad AF (2001) *Proc Natl Acad Sci USA* 98:5228–5233.
14. Adang MJ (2004) in *Handbook of Proteolytic Enzymes.* ed Barret AJ, Rawlings ND, Woessner JF (Elsevier Academic, New York), pp 296–299.
15. Darboux I, Nielsen-LeRoux C, Charles JF, Pauron D (2001) *Insect Biochem Mol Biol* 31:981–990.
16. Arca B, Lombardo F, Valenzuela JG, Francischetti IM, Marinotti O, Coluzzi M, Ribeiro JM (2005) *J Exp Biol* 208:3971–3986.
17. Zheng L, Whang LH, Kumar V, Kafatos FC (1995) *Exp Parasitol* 81:272–283.
18. Wilkins S, Billingsley PF (2001) *Insect Biochem Mol Biol* 31:937–948.
19. Ghosh AK, Ribolla PE, Jacobs-Lorena M (2001) *Proc Natl Acad Sci USA* 98:13278–13281.
20. Ito J, Ghosh A, Moreira LA, Wimmer EA, Jacobs-Lorena M (2002) *Nature* 417:452–455.
21. Devenport M, Fujioka H, Jacobs-Lorena M (2004) *Insect Mol Biol* 13:349–358.
22. Williamson MP (1994) *Biochem J* 297:249–260.
23. Sakaguchi K, Yanagishita M, Takeuchi Y, Aurbach GD (1991) *J Biol Chem* 266:7270–7278.
24. Lemos FJ, Cornel AJ, Jacobs-Lorena M (1996) *Insect Biochem Mol Biol* 26:651–658.
25. Feldmann AM, Billingsley PF, Savelkoul E (1990) *Parasitology* 101:193–200.
26. Xu X, Dong Y, Abraham EG, Kocan A, Srinivasan P, Ghosh AK, Sinden RE, Ribeiro JM, Jacobs-Lorena M, Kafatos FC, *et al.* (2005) *Mol Biochem Parasitol* 142:76–87.
27. Abraham EG, Pinto SB, Ghosh A, Vanlandingham DL, Budd A, Higgs S, Kafatos FC, Jacobs-Lorena M, Michel K (2005) *Proc Natl Acad Sci USA* 102:16327–16332.
28. Kennedy S, Wang D, Ruvkun G (2004) *Nature* 427:645–649.
29. Carter R, Miller LH, Rener J, Kaushal DC, Kumar N, Graves PM, Grotendorst CA, Gwadz RW, French C, Wirth D (1984) *Philos Trans R Soc London B Biol Sci* 307:201–213.
30. Han YS, Thompson J, Kafatos FC, Barillas-Mury C (2000) *EMBO J* 19:6030–6040.
31. Abdul-Rauf M, Ellar DJ (1999) *J Invertebr Pathol* 73:45–51.
32. Kalume DE, Okulate M, Zhong J, Reddy R, Suresh S, Deshpande N, Kumar N, Pandey A (2005) *Proteomics* 5:3765–3777.
33. Gobom J, Nordhoff E, Mirgorodskaya E, Ekman R, Roepstorff P (1999) *J Mass Spectrom* 34:105–116.
34. Perkins DN, Pappin DJ, Creasy DM, Cottrell JS (1999) *Electrophoresis* 20:3551–3567.
35. Falquet L, Pagni M, Bucher P, Hulo N, Sigrist CJ, Hofmann K, Bairoch A (2002) *Nucleic Acids Res* 30:235–238.
36. Eisenhaber B, Bork P, Eisenhaber F (1999) *J Mol Biol* 292:741–758.
37. Singh H, Raghava GP (2001) *Bioinformatics* 17:1236–1237.
38. Ifediba T, Vanderberg JP (1981) *Nature* 294:364–366.